# Computational Investigation on the Float-Type Flowmeter in Three-Dimensional Turbulence Flow Field


Xu Ying[a] Zhang Tao[a] Wang Huaxiang[a] Liu Zhengxian[b] Chen Deyu[c]

(a: College of Electric & Automation Engineering, Tianjin University 300072)

(b: College of Mechanical Engineering, Tianjin University 300072)

(c: Nanyang Technological University, Singapore)



**Abstract:** Based on the turbulence models and computational fluid dynamics (CFD), this paper presents a computational investigation on three-dimensional turbulence flow field of the float-type flowmeter. The forced floating element can be analyzed quantitatively from pressure field and the meter's flow rate from velocity field can be obtained. Meanwhile, this research is combined with an approach proposed by the authors, i.e. 'the error analysis method of the float-forced-balance-degree', which can realize a reliable estimate of the flow rate of the studied flowmeter. Simulation and experimental results show that the maximum full-scale error of flow rate is 3.4%, and the full-scale mean error, 1.77%. However, the corresponding errors using conventional design are 23.7% and 8.9% respectively.



**Keywords:** Float-Type Flowmeter, Turbulence, CFD, Float-Forced-Balance-Degree


## 1 Introduction

Generally, the research on the operating mechanism of float-type flowmeter (or variable area flowmeter, rotameter, suspended body flowmeter) is theoretically based on Bernoulli equation. Therefore it is impossible to get an exact value of viscous stress acting on the surface of float; certainly we cannot obtain a three-dimensional information of a flow field. In 1992, two German scholars, Bueckle.U and Durst.F first introduced CFD into the research of this kind of flowmeter, and they applied laser Doppler anemometry (LDA) to test the velocity distribution. It was proved that the test result was very similar to that of computation. However, their research was carried out on a glass tube flowmeter with longer geometrical size. In addition, the calculated flow field is laminar flow. Therefore they did not deal with the research of turbulent flow that widely exists in industry field.

In order to further investigate the detection mechanism of this type of flowmeter, a turbulence model combined with the CFD presented here is to discover the three-dimensional turbulence flow field. It will also lay the foundation for further studying their operational principle of other types of flowmeters.

## 2 Operating Principle of Floating Element Flowmeter

### 2.1 Detection Principle

The principle configuration of the floating element flowmeter is shown in the Fig.1. It mainly consists of a

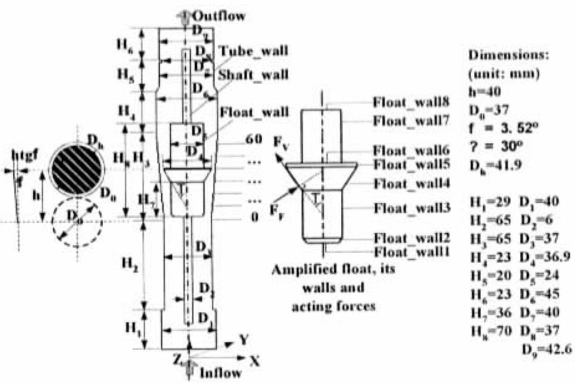


**Fig.1 Float-Type Flowmeter**

measuring tube and a floating element. There are four forces acting on the floating element, including the hydrodynamic force due to the flow, buoyancy ($F_b=V_f\rho g$), gravity($G=V_f\rho_f g$), viscous stress ($F_V$ generated by the friction between viscous liquid and walls of the float). Depending on the flow rate, the suspended body transiently takes up difference heights in the measuring tube, which results from the equilibrium among those forces. In the process of conventional analysis, the calculation of the viscous stress is ignored, and its influence is incorporated to the flow correction coefficient, which results in a certain error. The flow equation generally used is as follows.

$$Q_v = \alpha\pi\,[D_0 htg\,\phi + (htg\,\phi)^2]\sqrt{\frac{2gV_f(\rho_f-\rho)}{A_f\rho}} \quad (1)$$

**2.2 Modeling and Fluid State Analysis**

The conventional design method of float-type flowmeter is basically based on equation (1). For instance, the measured medium is supposed to be water at 20℃, in order to obtain a certain range of flow rate from 0.4~4 $m^3/h$, with the ratio of 10:1, equation (1) can usually be used to calculate the key structure size of the tapered tube and the float, as shown in figure 1. As a matter of experience, the value of the flow coefficient of this model is about 0.9~0.95. The flow field studied here is turbulence flow. The following CFD simulation will be done referring to the above data.

Here, Six calculation models having 25mm caliber flowmeter are designed, and the defined height location of the float in tapered tube is to be from 10mm to 60mm. One model is shown in fig. 1, in which the floating element is at the 40mm high in the tapered tube.

**2.3 Error Analysis Method of the Float-Forced-Balance-Degree**

In fact, if the initial or boundary conditions depends on those data mentioned above, CFD computation will result in a certain deviation when it tends to convergence. A phenomenon is observed that the composition of forces acting on the float is unbalanced after analyzing the computed pressure field of the object. Therefore, the authors put forward a novel method, i.e. the 'error analysis method of the float-forced-balance-degree', which can ensure the reliability of flow rate obtained from velocity field only when the balance situation of the forced float (including the gravity, buoyancy, hydrodynamic force due to the flow and viscous stress) is correct.

The pressure $F_F$ on the float can be obtained from the pressure field, its direction being vertical to each surface of the float( as shown in figure 1), the superposition of the Z-axis projection, $F_{F\uparrow}$, is

$$F_{F\uparrow} = \sum_{N=1}^{N=8}\left(\int_{S_N} P_N dS_N\right)\bullet\sin\theta_N = \sum_{N=1}^{N=8} f_N \bullet \sin\theta_N \quad (2)$$

The sum of hydrodynamic force due to the flow $F_P$ and buoyancy $F_b$ is $F_{F\uparrow}$, that is

$$F_{F\uparrow}=F_P+F_b. \quad (3)$$

The direction of the viscous friction force on the float surface is parallel with the float surface (as shown in figure 1), the superposition of the z-axis projection is

$$F_{V\uparrow} = \sum_{N=1}^{N=8} F_{VN} \bullet \cos\theta_N \quad (4)$$

Therefore, the sum of the force on the float in Z-axis direction obtained from the CFD is

$$F_{Total\uparrow} = \sum(F_{F\uparrow} + F_{V\uparrow}) \quad (5)$$

Here, the error formula of the float-forced-balance-degree is defined as

$$E_f = \frac{G - F_{Total\uparrow}}{G} \times 100\% \quad (6)$$

It can be seen that the smaller the absolute value $E_f$ is, the better the equilibrium degree, and it is generally considered that the numerical calculation will reach a reasonable accuracy until the absolute value of $E_f$ is less than 5%.

## 3 Mesh Generation and Calculation Initial Conditions

Based on turbulence model to solve the practical engineering problems, a simpler and widely used model is the standard K-ε model, and it is also adopted here. Discretization of the governing equations is based on the finite volume methodology (FVM), and the second-order upwind differential scheme is selected.

**3.1 Mesh Generation**

In the process of solving these discretized equations,SIMPLE algorithm, is applied.

The dissecting schemes of and the overall profile in axis direction of

**Fig.2 Computational meshes**

the flowmeter are shown fig2. Comparing the arrangements of computational meshes among the upstream, downstream and middle (tapered tube) of the flowmeter, the density of the grids in the middle is thicker, then, the up one and the down one in turn; the thickest section is at the smallest annular gap of the tapered space. It can be considered that this method will be more efficient for the simulation.

### 3.2 Calculation Conditions

The fluid medium is water at 20℃, whose density and viscosity are 998.2 $Kg/m^3$ , and 0.001003 Kg/ms, respectively. The material of all the walls (tube, float, pilot bar) is stainless steel (1Cr18Ni9Ta) and the wall roughness is to be 0. Being up to the conservation of mass, the outlet velocity could be partially unilaterally treated and obtained using extrapolation method from the inner nodes. Standard wall function [6-7] is adopted for the viscous layer adjacent to the solid wall. Corresponding to the float position, which is from 10mm to 60mm, the amplitudes of inlet flow velocity are listed in table 1 and the flow direction is shown in figure 1 as the arrowed direction. Based on the conventional methodology, the flow rate, the inlet velocities, which include the average velocity, U, and the maximum velocity, $U_{max}$ (Referring to J.Nikuradse's theory on the distribution of turbulence velocity of smooth tube [7]) are given in table 1. Meanwhile the velocity $U_S$ based on CFD computation is also given. Firstly, CFD is carried out based on the U and $U_{max}$. Then if the error of the float-forced-balance-degree is larger than 5% until convergence, the computation should be done again by gradually adjusting the amplitude of inlet flow velocity. Finally, a reasonable initial inlet flow velocity can be obtained. The computing and processing steps are described in part 4. Other boundary conditions, such as turbulence kinetic energy, turbulence dissipation rate, turbulivity, turbulence viscosity ratio and hydraulic diameter, are listed in the table 1 [7].

**Table 1 Calculation conditions**

| *H (mm)* | *Q* $(m^3h^{-1})$ | *Inlet Velocity* $(ms^{-1})$ | | | *K* $(m^2s^{-2})$ | $\varepsilon$ $(m^2s^{-3})$ | *I* % | $\mu_t/\mu$ | *L* (mm) |
|---|---|---|---|---|---|---|---|---|---|
| | | *Average* $U$ | *Maximum* $U_{max}$ | *Computational* $U_S$ | | | | | |
| 10 | 0.6032 | 0.13334 | 0.170024 | 0.145 | 8.8892E-5 | 0.001333 | 0.34 | 53．3 | 50 |
| 20 | 1.23234 | 0.27241 | 0.34386 | 0.31 | 3.7103E-4 | 0.00124 | 0.34 | 108.96 | 50 |
| 30 | 1.88743 | 0.41721 | 0.52485 | 0.511 | 8.7033E-4 | 0.00682 | 0.67 | 166.89 | 50 |
| 40 | 2.56846 | 0.56775 | 0.71346 | 0.724 | 0.00161 | 0.02338 | 0.67 | 227.110 | 50 |
| 50 | 3.27543 | 0.72409 | 0.90984 | 0.985 | 0.0040000 | 0.144 | 1 | 289.61 | 50 |
| 60 | 4.00835 | 0.88604 | 1.11343 | 1.2 | 0.0058887 | 0.3121 | 1 | 354.42 | 50 |

## 4 The Design of the Software flowchart Program

The software flowchart program is shown in Fig3.

① Based on the different position of the float (10mm~60mm), six models of computational meshes have been built individually;

② Iterative computation accuracy using SIMPLE algorithm is to be $10^{-4}$;

③ In order to improve convergence speed and computation accuracy, it is useful to increase the mesh density properly. Especially when the float lies in lower position (e.g. 10mm or 20mm high) inside the tapered tube, it is more important to gradually generate denser meshes around the zone of the biggest diameter of the float. Practice shows that such an arrangement can improve convergence speed and the accuracy;

④ When $E_f$ <=5% (Refers to the equation (6)), it can reach the aim of the simulation experiments. When $E_f$>5%, and if the grids density is suitable, the inlet flow velocity needs to be modified until the value of $E_f$ is satisfied.

## 5 Computed Results

### 5.1 Computed Pressure Field

For simplicity, here, only three figures about the computed results have been provided while the float is situated at 10mm, 40mm, and 60mm high in tube respectively. The contours of pressure field are shown in

Fig4. Its coordinate system is Z-Y plan and the unit is Pascal. From up to down, represented as from red to blue color, the bar on the left shows the tendency of pressure change. It can

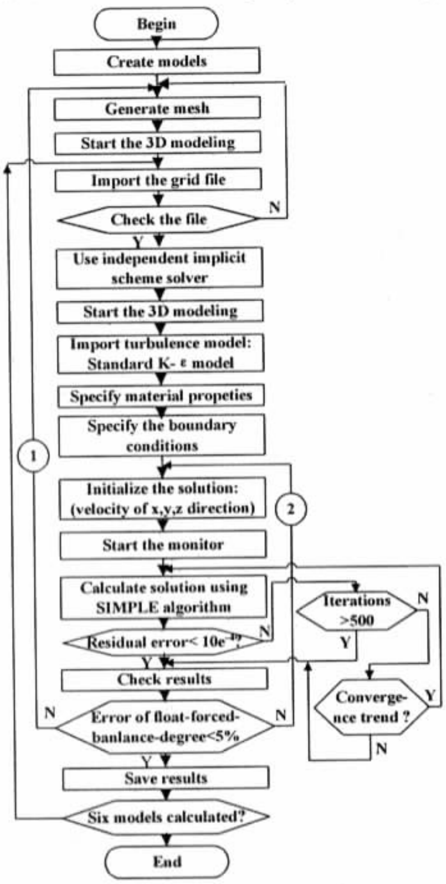


**Fig. 3. Simulation Flowchart**

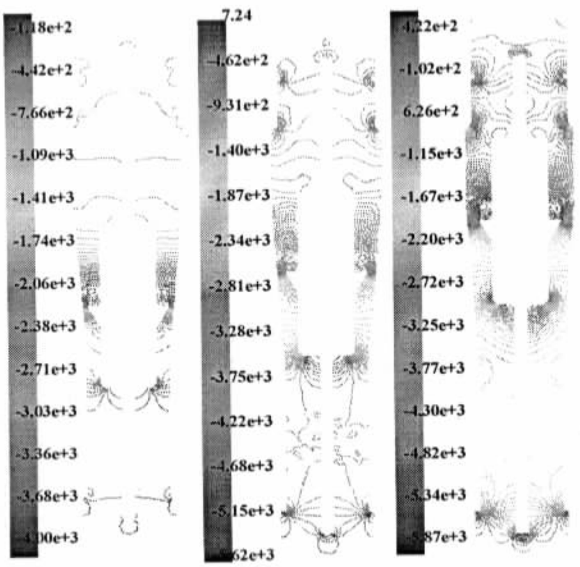

**Fig. 4 Contours of pressure (unit: Pascal)**

be analyzed from the figure as follows:

Comparing the absolute values of pressure, it can be seen that the intensity in downstream is higher than that in upstream; The highest value is around the corner of the biggest diameter of float in downstream; In the computed flow field, the higher position the float is situated at, the more obvious the intensity change in gradient is.

**5.2 Computed Velocity Field**

The vector-graph of partial velocity field is shown in Fig5. The coordinate system of view locates on the z-y plane, and velocity unit is m/s. From up to down, represented as from red to blue color, the bar shows that the velocity is decreasing. corresponding their vector–graphs. It can be analyzed from these figures as follows:

The velocity of the flow field is the most violent in the least circulation area of annular gap. In downstream, there exist turbulent eddies in the corner around the float surface. The higher position of float is situated at, the more obviously the eddies presented.

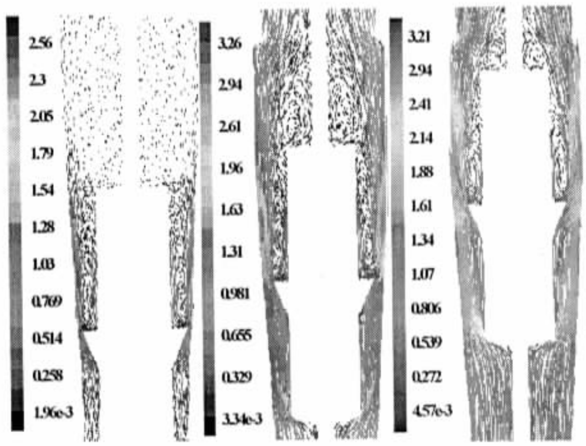

**Fig. 5 Vector-graphs of Velocity Field (unit: m/s)**

**5.3 Error Analysis of the Float-Forced-Balance-Degree**

**Table 2 Data Analysis**

| *h* mm | *Analysis of force on float*($G_f$=2.44956) N | | $E_f$ % | $V_h$ $ms^{-1}$ | $Q_S$ $m^3h^{-1}$ |
|---|---|---|---|---|---|
| | $F_{F\uparrow}$ | $F_{V\uparrow}$ | | | |
| 10 | 2.48826 | 0.00098 | 1.62 | 2.1122 | 0.656 |
| 20 | 2.43434 | 0.00162 | -0.56 | 2.216 | 1.402 |
| 30 | 2.51149 | 0.00407 | 2.7 | 2.4161 | 2.312 |
| 40 | 2.35249 | 0.00508 | 2.7 | 2.5066 | 3.275 |
| 50 | 2.45209 | 0.0103 | 0.53 | 2.6808 | 4.456 |
| 60 | 2.44994 | 0.0154 | 1 | 2.6745 | 5.429 |

The whole detail information of pressure field and velocity field can be acquired by turbulence flow computational simulation based on the standard K- ε model.

Integrating the computed pressure and shear stress over the float surface, and projecting them to Z-axis direction, then the pressure, $F_{F\uparrow}$ and the viscous stress, $F_{V\uparrow}$, can be obtained. Furthermore, the corresponding errors, $E_f$, can be calculated using the analytical method of float-forced-balance-degree. The relative data of the six models are given in table 2.

**5.4 Velocity and Flow Rate**

Based on the information of velocity field, average velocity, $V_h$, in the smallest annular gap of each model can be obtained. According to flow formula, $Q_S=AV_h$, the flow rate, listed in Table 2, can be also calculated.

## 6 Experiment Research

In order to verify the computed results, a float-type flowmeter made from perspex shown in fig.6, has been specially designed during the process of experimental research, and the experiment has been carried out based on the flow standard facilities shown in fig.7, the high level water tower is used as a stable pressure system, the turbine flowmeter with an accuracy of 0.2% is chosen as a standard flowmeter, and the remainders are labeled in the figure. There are six calibration points, namely the float position, are equidistant each to each among the 10mm-60mm range. The process of calibration was carried out 5 times for positive & reversal travel respectively, 6 calibration points for one travel and 3 times for each point. The instantaneous flow rate of the turbine flowmeter had been recorded during the process of calibration. After detecting many times, the six average values are obtained and listed in Table 3, in which the flow rates based on CFD and conventional methodology respectively are also given.

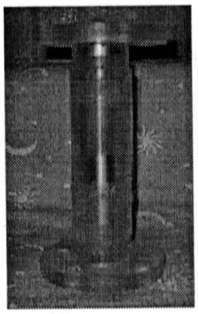

**Fig.6 Prototype**

- Comparing the experimental results, here, the formulas for error of reading and full-scale error of numerical results, $Err_S$, $Err_{SF}$, are defined as follows respectively:

$$Err_S = \frac{Q_S - Q_P}{Q_P} \times 100\% \qquad (11)$$

$$Err_{SF} = \frac{Q_S - Q_P}{Q_{PF}} \times 100\% \qquad (12)$$

- Comparing with the experiment, the formulas for error of reading and full-scale error of traditional design, $Err_D$, $Err_{DF}$, are also defined as follows:

$$Err_D = \frac{Q_D - Q_P}{Q_P} \times 100\% \qquad (13)$$

$$Err_{DF} = \frac{Q_D - Q_P}{Q_{PF}} \times 100\% \qquad (14)$$

It can be verified that the flow rate obtained by the simulation is quite close to that by the experiment. The maximal absolute full-scale error is 3.54% and its average absolute value is only 1.76%, which shows that a satisfied computational result can be obtained using the research method proposed in this thesis. However, using the conventional methodology, the corresponding error is 23.7% and 8.9%, respectively.

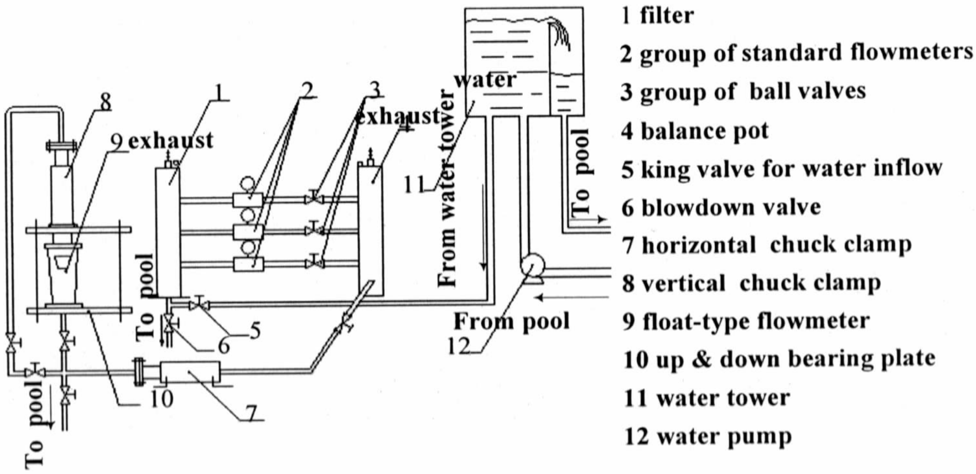


**Fig.7 Flow standard facilities**

**Table 3 Comparisons of experiment, computation and convention calculation**

| *Float position h (mm)* | *Experiment Flow rate* $Q_P\ m^3h^{-1}$ | *Computation Flow rate* $Q_S\ m^3h^{-1}$ | *Convention Flow rate* $Q_D\ m^3h^{-1}$ | *Errors of reading of computation* $Err_S$ % | *Full-scale errors of computation* $Err_{SF}$% | *Errors of reading of conventional calculation* $Err_D$% | *Full-scale errors of conventional calculation* $Err_{DF}$% |
|---|---|---|---|---|---|---|---|
| *10* | *0.68* | *0.65596* | *0.6032* | *-3.54* | *-0.458* | *-11.3* | *-1.463* |
| *20* | *1.382* | *1.40241* | *1.23234* | *1.477* | *0.388* | *-10.8* | *-2.85* |
| *30* | *2.205* | *2.31171* | *1.88742* | *4.84* | *2.03* | *-14.4* | *-6.05* |
| *40* | *3.155* | *3.2753* | *2.56846* | *3.813* | *2.29* | *-18.6* | *-11.2* |
| *50* | *4.350* | *4.45603* | *3.27543* | *2.438* | *2.02* | *-24.7* | *-20.5* |
| *60* | *5.250* | *5.42867* | *4.00835* | *3.403* | *3.40* | *-23.7* | *-23.7* |

## 7 Conclusions

Combination with the 'error analysis method of the float-forced-balance-degree' proposed by the authors, on the basis of turbulence models and CFD, here, the numerical investigation of the three-dimensional turbulence flow flied of the float-type flowmeter has been completed. The experimental measurement has been carried out based on the flow calibrating equipment with higher accuracy. By comparison from the point of view of flow rates, the computed results are found to agree well with the experimental measurements. It shows that the maximum of these full-scale errors is 3.54%, and the mean of them, 1.77%. While, the corresponding errors for the conventional method are 23.7% and 8.9% respectively.

Further more, the study on pressure field and the acquirements of pressure and viscous stress on the float surface can prove to be a good method for optimizing the shape of float, improving the design of this type of flowmeter, improving accuracy, extending measurement range. This method can also be of benefit to study on other fluid with higher viscous.

**Refrences**


1. Su Yanxun, Sheng Jian, Liang Guowei, 'Flow Measurement and Testing', Publishing company of Measurement of China, 1992.8
2. Bueckle, U.(Universitaet Erlangen-Nuernberg) Durst, F.|Howe, B.|Melling, A. Investigation of a floating element flowmeter. Source: Flow Measurement and Instrumentation v3 n4 Oct 1992 p215-225
3. *Bueckle, U.(Universitaet Erlangen-Nuernberg) Durst, F.|Koechner, H|Melling, A.* Further investigation of a floating element flowmeter. Source: Flow Measurement and Instrumentation Vol.6 No.1: pp.75-78 Jan 1995
4. *Barton, J.M. and Birt, S.F.*, "Numerical modeling of Three Dimensional Turbulent Jet Flows", AIAA Paper 800-808, 1980
5. *Launder, B.E. and Spalding, D.B.* The Numerical Computation of Turbulent Flows, Compute Methods in Applied Mech. And Eng., vol.3, No.1, 1974, pp.269-289
6. *Tao Wenshuan*, 'Numerical Method of Heat Transfer', Publishing Company of Xi'an Jiaotong University, China, 1988, 7
7. *Xu Ying*, 'Research on New-Style Smart Metal Tube Float Flowmeter', Dissertation of Tianjin University, 2002.6
8. *Zhang Zixong, Dong Zengnan, 'Viscosity fluid dynamics* ', Publishing company of Tsing Hua University, 1998,4